

RSC Advances



This is an *Accepted Manuscript*, which has been through the Royal Society of Chemistry peer review process and has been accepted for publication.

Accepted Manuscripts are published online shortly after acceptance, before technical editing, formatting and proof reading. Using this free service, authors can make their results available to the community, in citable form, before we publish the edited article. This *Accepted Manuscript* will be replaced by the edited, formatted and paginated article as soon as this is available.

You can find more information about *Accepted Manuscripts* in the [Information for Authors](#).

Please note that technical editing may introduce minor changes to the text and/or graphics, which may alter content. The journal's standard [Terms & Conditions](#) and the [Ethical guidelines](#) still apply. In no event shall the Royal Society of Chemistry be held responsible for any errors or omissions in this *Accepted Manuscript* or any consequences arising from the use of any information it contains.

Micropatterned model membrane with quantitatively controlled separation of lipid phases

Fumiko Okada ¹, Kenichi Morigaki ^{1,2*}

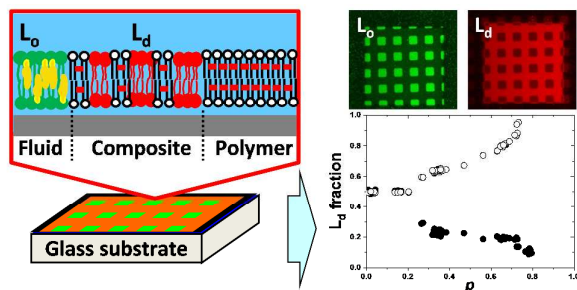
1: Graduate School of Agricultural Science, Kobe University, Rokkodaicho 1-1, Nada,
Kobe 657-8501 Japan

2: Research Center for Environmental Genomics, Kobe University, Rokkodaicho 1-1,
Nada, Kobe 657-8501 Japan

*Corresponding author:

Kenichi Morigaki: E-mail: morigaki@port.kobe-u.ac.jp, Fax: +81-78-803-5941

TOC entry:



A patterned model membrane of lipid rafts was generated by quantitatively controlling the separation of liquid-ordered and liquid-disordered bilayer domains.

Abstract

Localization of lipids and proteins in microdomains (lipid rafts) is believed to play important functional roles in the biological membrane. Herein, we report on a micropatterned model membrane that mimics lipid rafts by quantitatively controlling the spatial distribution of lipid phases. We generated a composite membrane of polymeric and fluid lipid bilayers by lithographic polymerization of diacetylene phospholipid (1,2-bis(10,12-tricosadiynoyl)-*sn*-glycero-3-phosphocholine: DiynePC). The composite membrane comprised polymer free-region (R_0), partially polymerized region (R_1), and fully polymerized region (R_2). As a ternary mixture of saturated lipid, unsaturated lipid, and cholesterol was introduced into the voids between polymeric bilayers, liquid-ordered (L_o) and liquid-disordered (L_d) lipid phases were accumulated in R_0 and R_1 , respectively. Local enrichment of L_d phase in R_1 (and L_o phase in R_0) was enhanced with a heightened coverage of polymeric bilayer in R_1 , supporting the premise that polymeric bilayer domains are inducing the phase separation. The pattern geometry (the area fractions of R_0 and R_1) also affected the enrichment due to the balance of gross L_o/L_d area fractions. Therefore, we could control the local L_o/L_d ratios by modulating the pattern geometry and polymer coverage in R_1 . Micropatterned model membrane with quantitatively controlled distribution of L_o/L_d phases offers a new tool to study the functional roles of lipid rafts by enabling to separate membrane-bound molecules according to their affinities to L_o and L_d phases.

1. Introduction

The cell membrane is made of a heterogeneous mixture of lipids and proteins. It is generally regarded that the lateral organization of membrane microdomains (“lipid rafts”) is closely related with the cellular functions.¹⁻⁴ The lateral heterogeneity is generated by the spontaneous segregation of lipids. Bilayer membranes containing saturated lipids, unsaturated lipids, and cholesterol spontaneously separate into the liquid-ordered (L_o) and liquid-disordered (L_d) phases in certain compositional regimes.^{5, 6} Phase separations in model membranes such as giant unilamellar vesicles (GUVs) and substrate-supported phospholipid bilayers (SPBs) have been extensively studied as models of lipid rafts.⁷⁻¹⁰ Studies using model membranes have provided important insight into the formation and physicochemical properties of lipid rafts.⁴

In the case of SPBs, micropatterning techniques have been applied to generate arrayed patches of L_o and L_d phases in the model membranes.¹¹⁻¹⁶ For example, Yoon *et al.* accumulated L_o and L_d phases on a silicon substrate by locally modulating the surface curvatures. L_o and L_d phases were enriched on the flat and corrugated surfaces, respectively, due to the difference in bending energy.¹¹ Some other studies have also exploited the different bending energies of L_o and L_d phases to realize patterned accumulation.¹²⁻¹⁴ Alternatively, some studies utilized kinetic effects to realize a patterned phase separation by using photolithography and micro-fluidics.^{15, 16} Patterned L_o/ L_d phases with controlled size and spatial distribution would provide a model membrane for systematic *in vitro* parallel assays of the lipid-raft-related functions.

We have previously developed a methodology to create patterned L_o/ L_d phases by using

a composite membrane of polymeric and fluid lipid bilayers.¹⁷ The polymeric bilayer was lithographically generated from a diacetylene phospholipid by UV illumination.¹⁸ The density of polymeric bilayer domains could be locally modulated by applying varied UV doses and removing non-reacted monomers with a detergent solution (Figure 1(A)).^{19,20} As a fluid bilayer containing a mixture of saturated lipid, unsaturated lipid, and cholesterol was incorporated, saturated lipid and cholesterol (L_o domains) were enriched in the polymer-free region (R_0), whereas unsaturated lipid (L_d domains) was enriched in the partially polymeric region (R_1) (Figure 1(B) and (C)).¹⁷ A fluorescent phospholipid (TR-PE) was used as the marker of L_d phase.²¹ Selective binding of dye-conjugated cholera toxin subunit B (CTB-488) to a glycolipid (G_{M1}) was used to detect L_o phase.²² (Representative fluorescence micrographs of the phase separation process are shown in Supporting Information (Figure S1).) We inferred that the driving force of the patterned L_o/L_d phase separation was the local bending of fluid bilayer at the boundary with polymeric bilayer, since a slight mismatch of the thickness is expected between polymeric and fluid bilayers.¹⁷ Due to the higher energetic penalty of bending, L_o domains are expected to be excluded from the boundaries, resulting in the accumulation of L_d domains around polymeric bilayer domains.^{23,24}

In the present work, we report that we can generate a micropatterned membrane with quantitatively controlled local L_o/L_d ratios. Although a number of techniques have been reported for patterning L_o/L_d phases, previous studies, including our work, have shown only qualitative separation of L_o and L_d phases. However, quantitatively controlled distribution of L_o/L_d phases and associated molecules in pre-designed patterns would be desirable for quantitatively evaluating the functional roles of lipid rafts. We

established a methodology to modulate the local L_o/L_d ratios through two experimentally controllable parameters. The first parameter is the area fractions of partially polymeric and polymer-free regions in the pattern. The second parameter is the area fraction of polymeric bilayers *within* the partially polymeric bilayer region. Well-defined separation of L_o and L_d phases should offer a new tool to study the functional roles of lipid rafts by enabling to separate membrane-bound molecules according to their affinities to L_o and L_d phases.

2. Materials and methods

2.1 Materials

1,2-bis(10,12-tricosadiynoyl)-*sn*-glycero-3-phosphocholine (DiynePC), 1,2-dioleoyl-*sn*-glycero-3-phosphocholine (DOPC), Sphingomyelin (Egg, chicken) (SM), cholesterol (ovine wool) (Chol), and G_{M1} ganglioside (brain, ovine) (G_{M1}) were purchased from Avanti Polar Lipids (Alabaster, AL). Texas Red 1,2-dihexadecanoyl-*sn*-glycero-phosphoethanolamine (TR-PE) and cholera toxin subunit B-Alexa Fluor 488 conjugate (CTB-488) were purchased from Molecular Probes (Eugene, OR). Bovine serum albumin (BSA) was purchased from Sigma-Aldrich (St. Louis, MO). Sodium dodecyl sulfate (SDS), glucose oxidase, catalase, and glucose were purchased from Nacalai Tesque (Kyoto, Japan). Deionized water used in the experiments was ultrapure Milli-Q water (Millipore) with a resistance of 18.2 MΩcm. It was used for cleaning substrates, preparing buffer solution (0.01 M sodium phosphate buffer with 0.15 M NaCl, pH 6.6 (PBS)) and all other experiments.

2.2 Substrate cleaning

Microscopy cover slips (Matsunami, Osaka, Japan) were used as substrates for bilayer deposition. The substrates were cleaned in an SDS solution (0.1 M) for 20 min under sonication, rinsed with Milli-Q water, treated in a solution of NH₄OH (28%)/ H₂O₂ (30%)/ H₂O (0.05:1:5) for 10 min at 65 °C, rinsed extensively with Milli-Q water, and then dried in a vacuum oven for 30 min at 80 °C. Before use, these substrates were further cleaned by the UV/ ozone treatment for 20 min (PL16-110, Sen Lights, Toyonaka, Japan).

2.3 Preparation of patterned polymeric bilayers

Bilayers of monomeric DiynePC were deposited onto glass substrates by the spontaneous spreading of vesicles. DiynePC powder was suspended in Milli-Q water by freezing in liquid nitrogen and thawing at 60 °C (five cycles). After the freeze-and-thaw, DiynePC suspension was homogenized by an ultrasonic homogenizer (Branson Sonifier150) at 60 °C (30 s x 2). Monomeric DiynePC suspension was applied onto a cleaned substrate on ice to immediately cool the membrane. (We previously discovered that it is important to deposit monomers at a low temperature for generating homogeneous DiynePC bilayers.²⁵)

Polymerization of DiynePC bilayers was conducted by UV irradiation using a mercury lamp (UVE-502SD, Ushio, Tokyo, Japan) as the light source. A closed system that comprised a water reservoir, a pump, and a cell (ca. 4 mL volume) was used. The water reservoir was depleted of oxygen by purging with argon.¹⁹ Oxygen-free water was circulated continuously by the pump through the cell where polymerization of the bilayers was conducted. The cell had two walls on the opposite sides, one being the sample (the SPB was inside the cell) and the other being a quartz window through which UV light was illuminated. Desired patterns were transferred onto the SPB in the polymerization process by illuminating the sample through a mask (a quartz slide with a patterned chromium coating) which was placed directly on the SPB. After sufficient circulation of deaerated water (typically for 15 minutes), the pump was stopped and the polymerization was started. The applied UV intensity was typically 7 mW/cm² at 254 nm and the UV dose was varied by changing the illumination time. After the UV irradiation, non-polymerized DiynePC molecules were removed from the substrate

surface by immersing in 0.1 M sodium dodecylsulfate (SDS) solution at 30 °C for 30 min and rinsing with Milli-Q water extensively. The polymerized bilayers were stored in Milli-Q water in the dark at 4 °C.

The patterned membrane consisted of polymer-free region (R_0), partially polymeric region (R_1), and fully polymerized region (R_2) (Figure 1). These patterns were generated by the successive UV exposure of monomeric membrane using two different photomasks (100 μm squares/ 8 μm circles or 10 μm squares). We varied two experimental parameters to modulate the phase separation. First, the area fractions of R_0 and R_1 (A_0 and A_1 : $A_0 + A_1 = 1$) were varied by changing the pattern geometries. Second, the fraction of the polymeric bilayer in R_1 (p) was changed by the applied UV dose for polymerization. These parameters are schematically summarized in Supporting Information (Figure S2).

2.4 Preparation of vesicle suspensions

Two types of vesicle suspensions were prepared: (a) DOPC with TR-PE (1mol%) (b) DOPC/SM/Chol (1:1:1) with G_{M1} and TR-PE (1mol% each). Lipids dissolved in organic solvents (DOPC, SM, Chol, and TR-PE were dissolved in chloroform, and G_{M1} was dissolved in methanol) were mixed in a round-bottom flask, dried with nitrogen (15min), and subsequently evaporated for at least 4 h in a vacuum desiccator. The dried lipid films were hydrated in PBS containing 3 mM CaCl_2 overnight (the total lipid concentration was 1 mM). Lipid membranes were dispersed by five freeze/thaw cycles, and the suspension was extruded by using a Liposofast extruder (Avestin, Ottawa, Canada) with 100 nm polycarbonate membrane filter (10 times) and 50 nm polycarbonate filter (15 times).

2.5 Phase separation of fluid bilayer in a patterned membrane

Fluid bilayers were incorporated into the voids between polymeric bilayers in a micropatterned membrane by spontaneous spreading of vesicles.^{26, 27} A droplet of vesicle suspensions (100 μ L) was put on a petri-dish and covered with a substrate having a patterned polymeric bilayer. The substrate was incubated for 30 minutes to allow complete spreading of SPBs on the patterned membrane. Excess vesicles were rinsed off by extensively flushing the substrate surface with Milli-Q water.

We first incorporated DOPC/ TR-PE into the patterned membrane to estimate the area fraction of the polymeric bilayer in R_1 (p). After the fluorescence microscopy observation, DOPC/ TR-PE was removed by immersing the sample in 0.1M SDS at 30 °C for 30 min and extensively rinsing with Milli-Q water. Subsequently, DOPC/SM/Chol (1:1:1) with G_{M1} and TR-PE (1mol% each) was introduced into the voids and incubated at 25 °C for 1-3 days. (Although phase separation started immediately after the introduction of fluid bilayer, we waited long enough to complete the phase separation.¹⁷) After the completion of phase separation, we observed the same positions of patterned membrane.

2.6 Fluorescence microscopy observation

Fluorescence microscopy observations were performed using an upright microscope (BX51WI, Olympus, Tokyo, Japan) equipped with a xenon lamp (UXL-75XB, Olympus), a 20x objective (NA 0.95), and a CCD camera (DP30BW, Olympus). Two

types of filter sets were used: 1) excitation 470-490 nm/ emission 510-550 nm (green fluorescence), 2) excitation 545-580 nm/ emission > 610 nm (red fluorescence). Fluorescence images were processed with the MetaMorph program (Molecular Devices, Sunnyvale, CA).

3. Results

We studied L_0/L_d phase separation in the patterned membranes with defined geometry and density of polymeric bilayer domains. Figure 2 shows the fluorescence micrographs of three patterned membranes comprising polymer-free region (R_0), partially polymeric region (R_1), and fully polymeric region (R_2). The large squares (100 μm) contained R_1 and small windows of R_0 (10 μm squares or 8 μm circles). Outside of the large squares was R_2 . The area fractions of R_0 (A_0) and R_1 (A_1) were varied by using photomasks with different geometries (A_0 and A_1 are the area fractions within R_0 and R_1 ($A_0 + A_1 = 1$)). (R_2 is not included in calculating the area fractions, because we assume that fluid bilayers are excluded from it.) A_0/A_1 was 0.25/ 0.75 for the pattern (A), and 0.05/ 0.95 for the patterns (B) and (C), respectively. The polymeric bilayer fraction in R_1 (p) was varied by changing the applied UV dose. To estimate the values of p , we first incorporated a fluid bilayer that did not separate into two phases (DOPC/ TR-PE) (upper panels of Figure 2). The fluorescence intensity of TR-PE in R_0 (I_0^{TR}) was higher than that in R_1 (I_1^{TR}) due to the fact that R_1 was partially covered by polymeric bilayer. The values of p were estimated with the following equation, assuming that TR-PE is uniformly distributed in the fluid bilayer (I_0^{TR} and I_1^{TR} represent the *true* fluorescence intensities after subtracting the background fluorescence intensity from the measured intensities):²⁰

$$p = 1 - (I_1^{TR} / I_0^{TR}). \quad (3)$$

The obtained p values are given in Figure 2. After evaluating the p values, we removed DOPC/ TR-PE with a detergent solution (0.1M SDS, 30 min at 30 °C: this treatment did

not alter polymeric bilayer domains²⁰) and incorporated a new lipid membrane (DOPC/ SM/ Chol (1:1:1)) that separated into L_o and L_d phases. The membrane contained TR-PE and G_{MI} (1mol% each). After incubation, TR-PE was enriched in R_1 , as evidenced by the higher fluorescence intensity in R_1 compared with R_0 , in spite of the fact that there was less fluid membrane in R_1 (note the inverted contrast between the upper and middle panels). Fluidity of the membrane in R_1 was confirmed by the fluorescence recovery after photobleaching (FRAP) measurements (Supporting Information, Figure S3). After observing the distribution of TR-PE, we added CTB-488 to detect L_o phase. CTB-488 was preferentially found in R_0 (lower panels). The line profiles of fluorescence intensities confirmed the inverted accumulation of TR-PE and CTB-488 (Supporting Information, Figure S4). Comparing the middle panels of (B) and (C), we note that the fluorescence intensity of TR-PE in R_1 was higher for the sample having a larger p (C). Concomitantly, the fluorescence of CTB-488 in R_0 was more prominent in this sample (bottom panel). These observations suggested that a higher density of polymeric bilayer in R_1 enhanced the patterned separation of L_o and L_d phases. The local enrichment of TR-PE and CTB-488 was evaluated from the fluorescence intensities in R_0 and R_1 (I_0^{TR} , I_1^{TR} , I_0^{CTB} , I_1^{CTB}) using the following equations (the background fluorescence intensities were subtracted from the measured intensities to obtain the *true* fluorescence intensities of TR-PE and CTB-488):

$$\text{Enrichment of CTB-488 in } R_0: \quad D_0^{CTB} = (I_0^{CTB} / I_1^{CTB}) (1-p). \quad (4)$$

$$\text{Enrichment of TR-PE in } R_1: \quad D_1^{TR} = (I_1^{TR} / I_0^{TR}) / (1-p) \quad (5)$$

The fluorescence intensity in R_1 was normalized with the area fraction of fluid bilayer

($1-p$), considering the fact that the region contained less fluid bilayer due to polymeric bilayer. The obtained values of D_I^{TR} and D_0^{CTB} are given in Figure 2. Enrichment of L_o and L_d phases in R_0 and R_1 was enhanced for a sample with a higher p value ((B) and (C)).

To evaluate the effects of polymeric bilayer on the phase separation, we measured the enrichment of TR-PE and CTB-488 (D_I^{TR} and D_0^{CTB}) in samples with systematically varied p . (We generated patterned samples with varied UV doses to obtain different p values.) The two pattern geometries shown in Figure 2 ($A_I = 0.75$ and $A_I = 0.95$) were used. The plot of D_I^{TR} versus p is summarized in Figure 3(A). D_I^{TR} increased with the p value. For low p values, D_I^{TR} was close to 1, as expected, and increased gradually with p . The increase was more prominent for higher p values. In the case of the membrane with $A_I = 0.95$, D_I^{TR} increased very steeply as the p value exceeded 0.7 (Figure 3(A)). The plot of D_I^{CTB} versus p also shows that more CTB-488 molecules are localized in R_0 for a higher p value (Figure 3(B)). The data for CTB-488 were rather scattered, presumably due to the effects of non-specific adsorption, although we suppressed it by applying a blocking agent (BSA). These results clearly show that the patterned phase separation is positively correlated with the amount of polymeric bilayer domains.

Localization of TR-PE and CTB-488 in the patterned membranes reflects the accumulation of L_d and L_o phases in R_1 and R_0 , respectively. We estimated the occupied area fractions of L_d phase in R_0 and R_1 (a_0^{Ld} and a_I^{Ld}) from the observed enrichment of TR-PE in R_1 , assuming the following two conditions. First, we assumed that the gross area fractions of L_o and L_d phases were 0.5 (equal area of the two phases) for the lipid

composition used (DOPC/ SM/ Chol = 1:1:1), as previously estimated by the atomic force microscopy observations.²⁸ Second, we assumed that the area fraction of L_d phase was proportional to the fluorescence intensity of TR-PE, since TR-PE was predominantly partitioned in the L_d phase. By applying these boundary conditions to the experimentally obtained enrichment of TR-PE in R_1 (D_I^{TR} in Figure 3(A)), we could calculate the area fractions of L_o / L_d in R_0 and R_1 (Eqs. (6)-(8)).

$$\text{Enrichment of } L_d \text{ phase in } R_1: \quad a_I^{Ld} = D_I^{TR} a_0^{Ld}. \quad (6)$$

The total areas of L_d domains after the phase separation should be equal to the gross area of L_d phase:

$$(1 - A_I) a_0^{Ld} + A_I D_I^{TR} a_0^{Ld} (1 - p) = 0.5 \{(1 - A_I) + A_I (1 - p)\}. \quad (7)$$

From the equations (6) and (7), the area fraction of L_d phase in R_0 can be calculated as follows:

$$a_0^{Ld} = 0.5 (1 - A_I p) / \{(1 - A_I) + A_I D_I^{TR} (1 - p)\}. \quad (8)$$

The estimated area fractions are shown in Figure 4. For $A_I = 0.75$, a_0^{Ld} decreased and a_I^{Ld} increased progressively with p , indicating enrichment of L_o and L_d phases in R_0 and R_1 , respectively. On the other hand, in the case of $A_I = 0.95$, a_0^{Ld} decreased with p , whereas a_I^{Ld} increased only slightly, indicating that R_0 consisted mostly of L_o phase, whereas R_1 remained a mixture of L_o and L_d phases. This asymmetric enrichment can be understood by considering the fact that R_0 is much smaller compared with that of R_1 ($A_0 = 0.05$ and $A_I = 0.95$). As a consequence, a part of the L_o phase should have remained in

R_1 , even if R_0 was highly enriched with L_o phase.

The results in Figures 4 demonstrate that we can quantitatively control the local L_o/L_d ratios in a patterned membrane by the pattern geometry (area fractions of R_0 and R_1) and the polymeric bilayer fraction in the partially polymeric region. This feature enables to create an array of model membranes with varied local L_o/L_d ratios. Figure 5 shows a patterned membrane that has four regions with different polymeric bilayer coverages, a polymer free region (a), two partially polymeric regions (b and c), and a fully polymeric region (d). By incorporating DOPC/ TR-PE, we could estimate the area fractions of polymeric bilayers in (b) and (c) to be 0.02 and 0.48, respectively (Figure 5(A)). Subsequently, we incorporated DOPC/ SM/ Chol (1:1:1) containing G_{MI} and TR-PE (1mol% each), and observed that TR-PE and CTB-488 were distributed in the three regions ((a) – (c)) according to the densities of polymeric bilayer domains. TR-PE was most accumulated in the region (c) where the density of polymeric bilayers was highest (except for the fully polymerized region (d)) (Figure 5(B)), whereas CTB-488 was most accumulated in the polymer-free region (a) (Figure 5(C)). (Enrichment of TR-PE at the boundaries between the regions (b) and (d) was caused presumably by the partial polymerization at the boundary of these regions.) From the fluorescence intensities of TR-PE, we evaluated the fractions of L_d phase in each region to be 0.24 (a), 0.34 (b), and 0.96 (c). (The L_o/L_d ratio could not be quantified in the fully polymeric region.)

4. Discussion

The local L_o/L_d ratios in the micropatterned membrane could be modulated by the pattern geometry and polymer density. Localization of molecules associated with L_o and

L_d phases in R_0 and R_1 was enhanced with a higher coverage of polymeric bilayer. This result supports the premise that patterned phase separation is induced by the accumulation of L_d domains around polymeric bilayer domains (Supporting Information, Figure S5). We made a model that assumed that the amount of L_d domains accumulated around polymeric bilayer domains was proportional to the area fraction of polymeric bilayers in R_1 (p). The model could qualitatively reproduce the experimentally observed increase of D_I^{TR} with p (Supporting Information, Figure S6). The consistency is a further support of the premise that we can control the L_o/L_d distributions by tuning the local area fractions of polymeric bilayer.

An important feature of the present micropatterning approach is the fact that polymeric and fluid bilayers are forming a continuous, two-dimensional composite membrane. Therefore, the phase separation is induced by the structural element (polymeric bilayer domain) embedded within the membrane. It is in contrast with other approaches which generally utilize the interactions of the membrane with the substrate surface for patterning L_o and L_d phases.¹¹⁻¹⁶ The fact that the present approach does not rely on the interaction with the substrate should allow us to construct a model membrane on a wider variety of substrates. In the future, it may be possible to detach the membrane from the substrate with a hydrophilic polymer cushion and suspend it in a similar fashion as black lipid membranes.^{29, 30}

There are also some technical limitations at present. The phase separation takes quite a long time to complete (several hours to several days). The rate is presumably limited by the slow diffusion of lipid domains on the glass substrate. It has been reported that

lateral diffusion of large domains is hindered due to the frictional drag on the substrate.³¹ Another important factor to be considered is the effect of embedded polymeric bilayers on the diffusion of membrane-bound molecules. Our previous studies have suggested that the lateral diffusion coefficients of lipids decreased proportionally with the polymer fraction.²⁰ The retarded diffusion may affect the distribution of membrane-bound molecules by the kinetic effects. These technical hurdles must be mitigated by optimizing the pattern geometry and the amount of polymeric bilayer. It is also important to note that information on the gross area fractions of L_o and L_d phases for the lipid composition used is needed to determine the L_o and L_d fractions in R_0 and R_1 from the experimentally observed distributions of marker molecules (e.g. TR-PE) (Figure 4). The L_o/L_d fractions have been mostly determined from the microscopic observation of giant vesicles.^{22,32} Since the L_o/L_d fractions may slightly vary for SPBs and giant vesicles due to the presence (or absence) of the solid support, the total area fractions should be evaluated using an SPB. The effects of polymeric bilayer domains on the phase behaviors of lipid membranes should be evaluated, as well.

In summary, a patterned composite membrane of polymeric and fluid bilayers can quantitatively control the local distribution of membrane-bound molecules according to their affinities to L_o and L_d phases. By changing the pattern geometry (R_0/R_1 area fractions) and polymeric bilayer coverage in R_1 , we can modulate the local L_o/L_d ratios with a designed pattern. A potential application of the patterned membrane should be to measure the partitioning of membrane-bound proteins to L_o and L_d phases. It is commonly conceived that the association of proteins with lipid rafts is playing important functional roles.^{33,34} Therefore, quantitative evaluation of protein

partitioning into lipid rafts is an important issue. Conventionally, enrichment in detergent-resistant membranes (DRMs) was used to evaluate the association of proteins with lipid rafts.^{35, 36} A more quantitative approach was recently developed by the microscopic observation of giant vesicles.^{37, 38} Micropatterned model membrane with controlled distribution of L_o/ L_d phases provides new possibilities to gauge the association of proteins to lipid rafts. Since patterned membranes are amenable to parallel analyses, it should significantly facilitate the determination process. Furthermore, we can construct an array of model membranes with multiple L_o/ L_d ratios, as shown in Figure 5. Such membranes may find various biomedical applications, including the separation of membrane bound molecules in combination with an electrophoretic or fluidic devices.

Acknowledgements

This work was supported by Grant-in-Aid for Scientific research from Japan Society for the Promotion of Science (#21651060, #22360022, #25286062). We thank Ms. Akane Nagao for the FRAP measurements.

Figures:

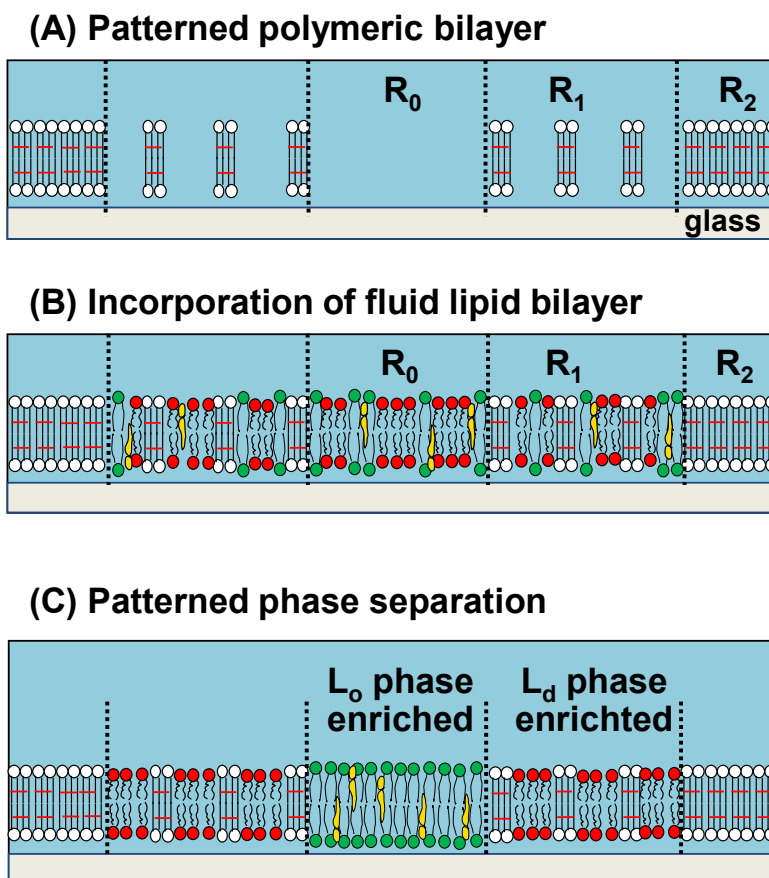


Figure 1: Schematic illustration of the patterned phase separation in a model membrane.

(A) The patterned membrane has three regions: polymer-free region (R_0), partially polymeric region (R_1), and fully polymeric region (R_2). As a mixed bilayer is introduced into the voids between polymeric bilayers (B), L_0 and L_d phases spontaneously accumulate in R_0 and R_1 , respectively (C).

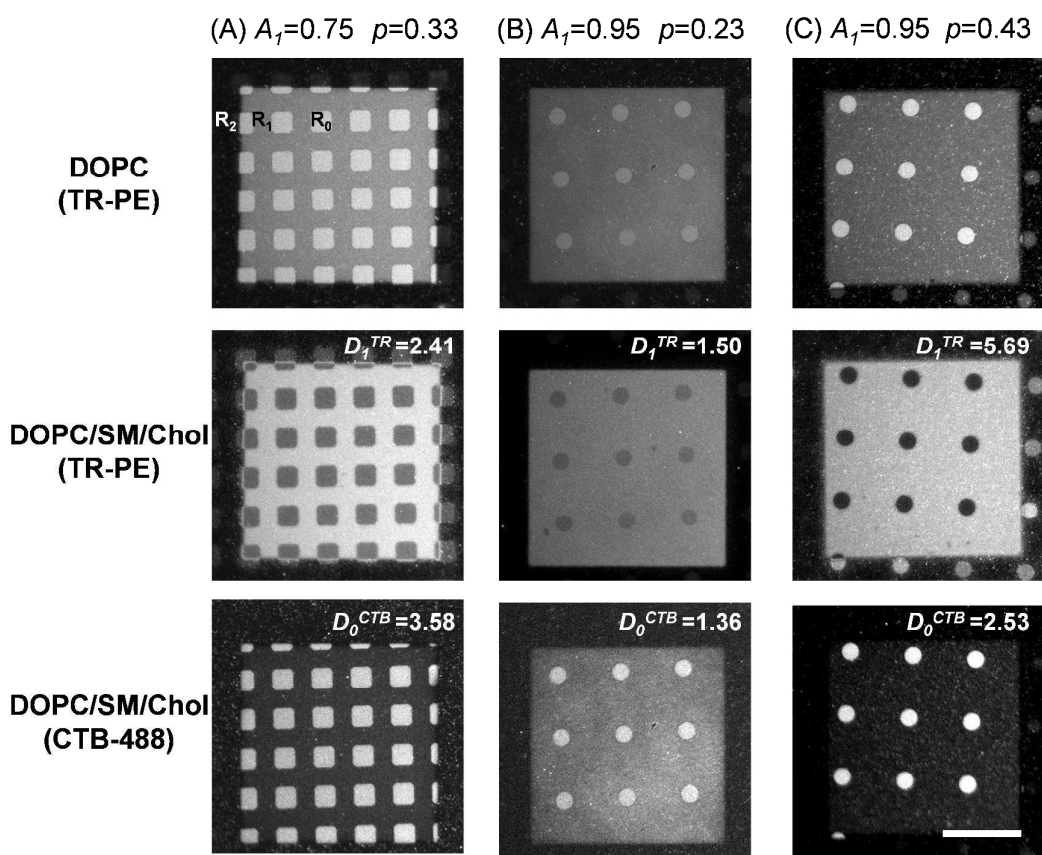


Figure 2: Fluorescence micrographs of the phase separation in patterned bilayers having different geometries and polymeric bilayer fractions: The area fractions of R_1 (A_1) (shown at the top) were varied by using different photomasks upon polymerization. The polymeric bilayer fractions in R_1 (p) (shown at the top) were determined by incorporating a homogeneous bilayer (DOPC/ TR-PE) (upper panel). Subsequently, the fluid bilayer was exchanged with a mixed lipid bilayer (DOPC/ SM/ Chol/ TR-PE/ G_{M1}) and the phase separation was observed using the markers of L_d and L_o phases (TR-PE and CTB-488) (middle and lower panels). The enrichment of TR-PE and CTB-488 in R_1 and R_0 (D_1^{TR} and D_0^{CTB}) were estimated from the fluorescence intensities (see the text). The scale bar is 40 μm .

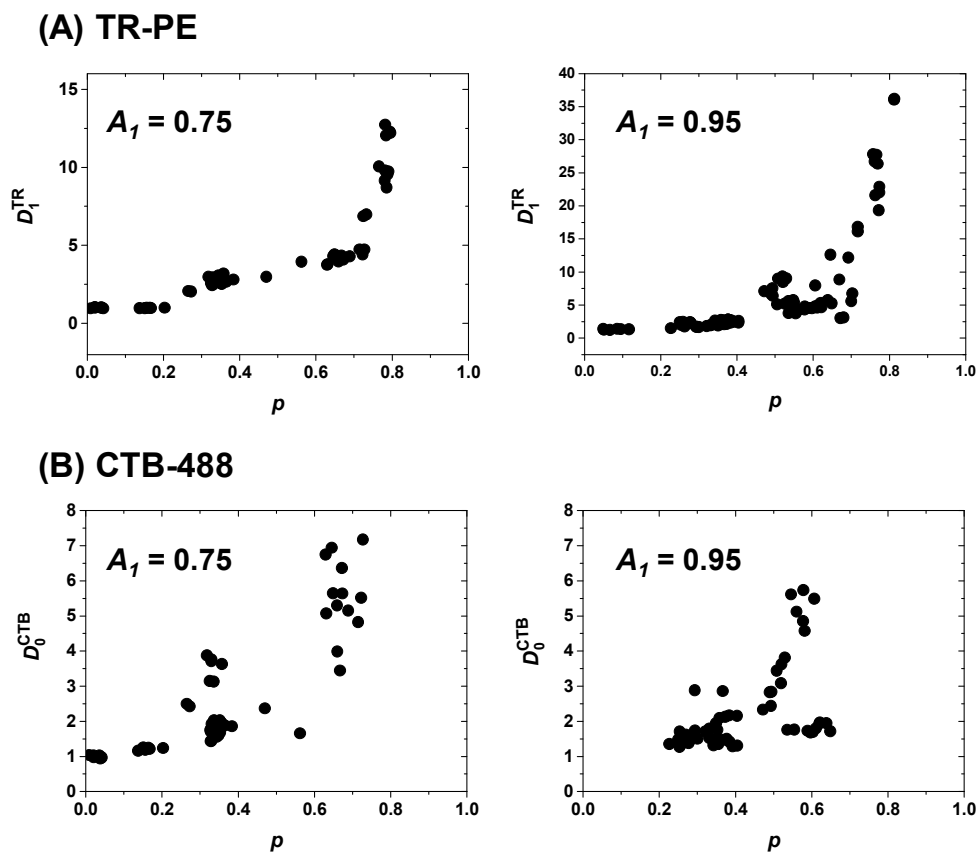


Figure 3: Enrichment of TR-PE in R_1 (D_1^{TR}) (A) and CTB-488 in R_0 (D_0^{CTB}) (B) in patterned samples with varied p . The two pattern geometries in Figure 2 ($A_1 = 0.75$ and 0.95) were used. Each data point represents the evaluation from a single fluorescence micrograph. Results from at least four independent samples were compiled.

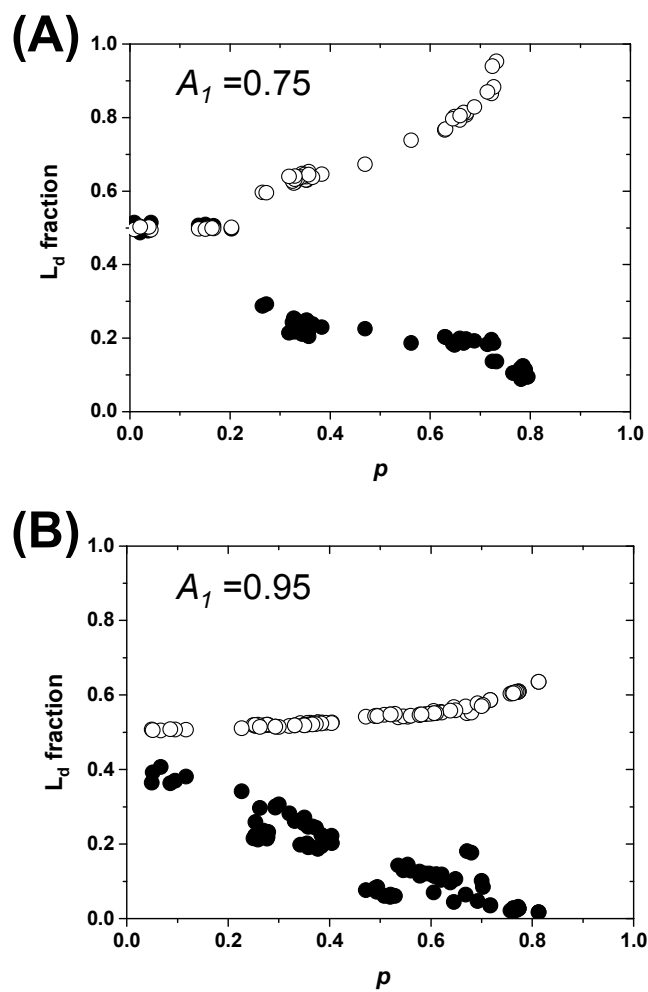


Figure 4: The area fractions of L_d phase in R_0 and R_1 were estimated from the enrichment of TR-PE in Figure 3(A). We assumed that the gross area fractions of L_0 and L_d phases were 0.5 for the lipid composition used. Open circles: L_d phase in R_1 ($a_1^{L_d}$); Filled circles: L_d phase in R_0 ($a_0^{L_d}$).

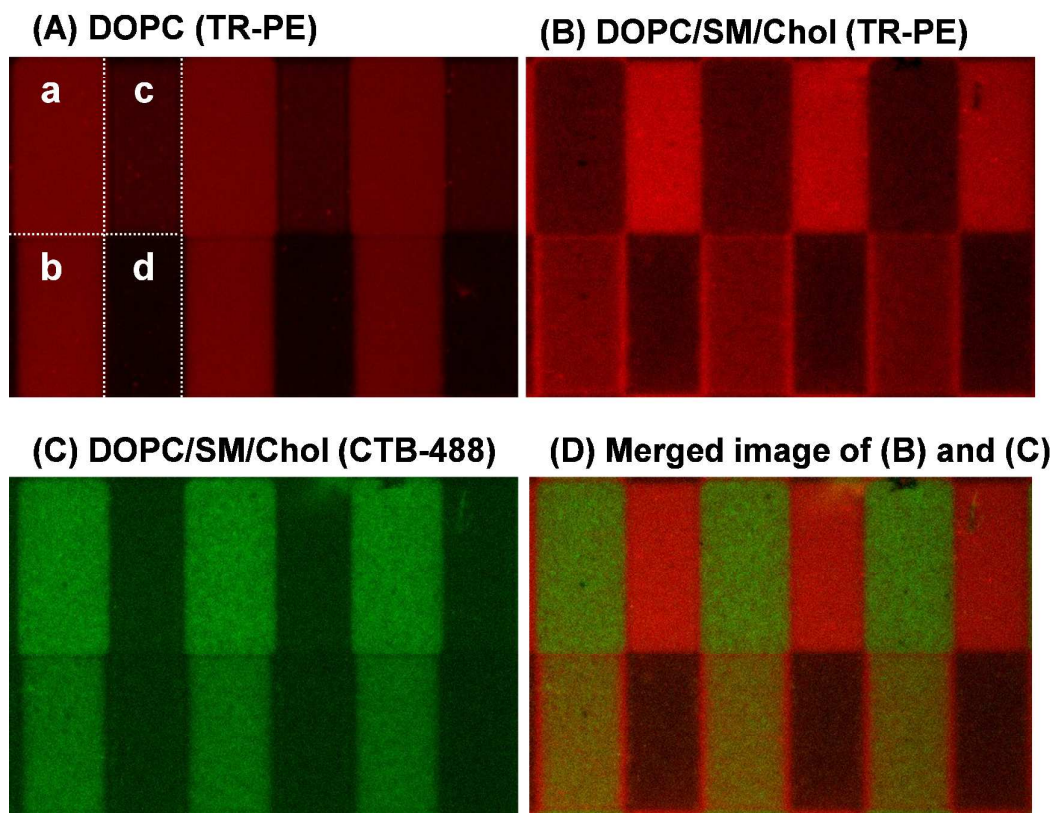


Figure 5: Phase separation in a patterned membrane with four different regions: The bilayer consisted of (a) polymer-free, (b) (c) partially polymeric ($p = 0.02$ and 0.49), and (d) polymeric regions. The patterned bilayer was first filled with a homogeneous bilayer (DOPC) to determine p (A). Subsequently, the fluid bilayer was exchanged with a mixed lipid bilayer (DOPC/ SM/ Chol/ TR-PE/ G_{M1}) and the phase separation was observed ((B)-(D)). The size of each region was $20 \times 10 \mu\text{m}$.

References:

1. K. Simons and E. Ikonen, *Nature*, 1997, **387**, 569-572.
2. K. Simons and D. Toomre, *Nature Rev. Mol. Cell Biol.*, 2000, **1**, 31-41.
3. K. Jacobson, O. G. Mouritsen and R. G. W. Anderson, *Nature Cell Biol.*, 2007, **9**, 7-14.
4. D. Lingwood and K. Simons, *Science*, 2010, **327**, 46-50.
5. D. Marsh, *Biochim. Biophys. Acta*, 2009, **1788**, 2114-2123.
6. G. W. Feigenson, *Biochim. Biophys. Acta*, 2009, **1788**, 47-52.
7. C. Dietrich, L. A. Bagatolli, Z. N. Volovyk, N. L. Thompson, M. Levi, K. Jacobson and E. Gratton, *Biophys. J.*, 2001, **80**, 1417-1428. .
8. S. L. Veatch and S. L. Keller, *Biophys. J.*, 2003, **85**, 3074-3083.
9. T. Baumgart, S. T. Hess and W. W. Webb, *Nature* 2003, **425**, 821-824.
10. J. M. Crane and L. K. Tamm, *Biophys. J.*, 2004, **86**, 2965-2979.
11. T.-Y. Yoon, C. Jeong, S.-W. Lee, J. H. Kim, M. C. Choi, S.-J. Kim, M. W. Kim and S.-D. Lee, *Nat. Mat.*, 2006, **5**, 281-285.
12. M. O. Ogunyankin, A. Torres, F. Yaghmaie and M. L. Longo, *Langmuir*, 2012, **28**, 7107-7113.
13. F. Roder, O. Birkholz, O. Beutel, D. Paterok and J. Piehler, *J. Am. Chem. Soc.*, 2013, **135**, 1189-1192.
14. E. L. Kendall, V. N. Ngassam, S. F. Gilmore, C. J. Brinker and A. N. Parikh, *J. Am. Chem. Soc.*, 2013, **135**, 15718-15721.
15. A. R. Sapuri-Butti, Q. Li, J. T. Groves and A. N. Parikh, *Langmuir*, 2006, **22**, 5374-5384.
16. L. Chao and S. Daniel, *J. Am. Chem. Soc.*, 2011, **133**, 15635-15643.
17. T. Okazaki, Y. Tatsu and K. Morigaki, *Langmuir*, 2010, **26**, 4126-4129.
18. K. Morigaki, T. Baumgart, A. Offenhäusser and W. Knoll, *Angew. Chem., Int. Ed.* , 2001, **40**, 172-174.
19. K. Morigaki, K. Kiyosue and T. Taguchi, *Langmuir*, 2004, **20**, 7729-7735.
20. T. Okazaki, T. Inaba, Y. Tatsu, R. Tero, T. Urisu and K. Morigaki, *Langmuir*, 2009, **25**, 345-351.
21. T. Baumgart, G. Hunt, E. R. Farkas, W. W. Webb and G. W. Feigenson, *Biochim. Biophys. Acta*, 2007, **1768**, 2182-2194.
22. N. Kahya, D. Scherfeld, K. Bacia, B. Poolman and P. Schwille, *J. Biol. Chem.*, 2003, **278**, 28109-28115.
23. P. I. Kuzmin, S. A. Akimov, Y. A. Chizmadzhev, J. Zimmerberg and F. S. Cohen, *Biophys. J.*, 2005, **88**, 1120-1133.

24. E. Evans and W. Rawicz, *Phys. Rev. Lett.*, 1990, **64**, 2094 - 2097.
25. K. Morigaki, H. Schönherr and T. Okazaki, *Langmuir*, 2007, **23**, 12254-12260.
26. R. P. Richter, R. Berat and A. R. Brisson, *Langmuir*, 2006, **22**, 3497-3505.
27. T. Okazaki, K. Morigaki and T. Taguchi, *Biophys. J.*, 2006, **91**, 1757-1766.
28. S. Chiantia, N. Kahya, J. Ries and P. Schwille, *Biophys. J.*, 2006, **90**, 4500-4508.
29. S. R. Garg, Juergen; Luedtke, Karin; Jordan, Rainer; Naumann, Christoph A., *Biophys. J.*, 2007, **92**, 1263-1270.
30. A. Orth, L. Johannes, W. Römer and C. Steinem, *ChemPhysChem*, 2012, **13**, 108-114.
31. E. Sackmann, *Science (Washington)*, 1996, **271**, 43-48.
32. S. L. Veatch and S. Keller, *Phys. Rev. Lett.*, 2005, **94**, 148101.
33. I. Levental, M. Grzybek and K. Simons, *Biochemistry*, 2010, **49**, 6305-6316.
34. I. Levental, D. Lingwood, M. Grzybek and Ü. Coskun, *Proc. Natl. Acad. Sci. U. S. A.*, 2010, **107**, 22050-22054.
35. S. Mayor and F. R. Maxfield, *Mol. Biol. Cell*, 1995, **6**, 929-944.
36. D. A. Brown and E. London, *J. Biol. Chem.*, 2000, **275**, 17221-17224.
37. N. Kahya, D. A. Brown and P. Schwille, *Biochemistry*, 2005, **44**, 7479-7489.
38. T. Baumgart, A. T. Hammond, P. Sengupta, S. T. Hess, D. A. Holowka, B. A. Baird and W. W. Webb, *Proc. Natl. Acad. Sci. U. S. A.*, 2007, **104**, 3165-3170.